

# Effects of Cross Wall to the System Stiffness of Deep Excavations in Clay

Zih Yun Wang<sup>1</sup>, Bin Chen Benson Hsiung<sup>2</sup>, Hsui-Sheng Hsieh<sup>3</sup> and Louis Ge<sup>4</sup>

<sup>1</sup>Department of Civil Engineering, National Taiwan University, Taipei, Taiwan

<sup>2</sup>Department of Civil Engineering, National Kaohsiung University of Applied Science, Kaohsiung, Taiwan

<sup>3</sup>Trinity Foundation Engineering Consultants, Co., Ltd., Taipei, Taiwan

<sup>4</sup>Department of Civil Engineering, National Taiwan University, Taipei, Taiwan

E-mail: louisge@ntu.edu.tw

**ABSTRACT:** In urban area with soft clay deposit, it is required that the diaphragm wall deflection of a deep excavation be limited to minimize damages to adjacent buildings. The auxiliary measures such as buttress wall, cross wall and ground improvement have been applied to deep excavation. The so-called three-dimensional effect accounts for the presence of buttress wall and cross wall as well as the size of the excavation area and depth. When considering the three-dimensional effect, the diaphragm wall deflection can be much reduced compared with its plane strain condition. This study uses three-dimensional finite element analysis, by means of PLAXIS 3D, to predict the wall deflection. The numerical results are compared with the outcome from a one-dimensional analysis and field measurements. In this study, the effect of auxiliary measures is incorporated into the system stiffness of the excavation, where the presence of auxiliary measures is given in form of increasing the undrained shear strength of the soil mass within the excavation zone. In turn, it leads to an increase of the factor of safety against basal heave and a reduction of the wall deflection. One case history in soft clay are presented in this paper to evaluate the effectiveness of the three-dimensional finite element analysis considering the effect of auxiliary measures.

**Keywords:** deep excavation, three-dimensional effect, wall deflection

## 1. INTRODUCTION

Diaphragm wall is a retaining system to retain the pit, protect adjacent buildings and prevents excessive ground movements during excavation. There are several methods of reducing wall deflections in deep excavation, such as buttress wall and cross wall. In this study a three-dimensional finite element program, PLAXIS 3D, was used to simulate the wall deformation during construction for an excavation with additional cross wall. The numerical results were compared with the results from the one-dimensional beam-spring model analysis and field measurements. The effects of cross wall are incorporated into the system stiffness by increasing the undrained shear strength of the soil mass within the excavation zone for beam-spring model stated above. The purpose of this paper is to evaluate the effectiveness of the real three-dimensional analysis and the one-dimensional analysis with consideration of system stiffness for an excavation with details stated above.

## 2. BACKGROUND

### 2.2 System stiffness

Clough et al. (1989) first presented the relationship between wall displacement, system stiffness and factor of safety against basal heave ( $F_b$ ). As shown in Figure 1, wall displacement is controlled by system stiffness and  $F_b$ . If the system stiffness is constant, as the value of  $F_b$  increases, the maximum wall displacement would significantly reduce. The factor of safety against basal heave,  $F_b$ , is calculated based on the equations defined by Terzaghi (1967). The Y-axis in Figure 1 is the ratio of the maximum wall displacement ( $\delta_{hm}$ ) to the excavation depth ( $H_e$ ), while the X-axis is the system stiffness ( $S$ ) defined by Clough et al. (1989) as follows.

$$S = \frac{EI}{r_w \cdot x h_{avg}^4} \quad (1)$$

Where  $EI$  is the flexural stiffness of the retaining wall,  $r_w$  is the unit weight of water, and  $h_{avg}$  is the average vertical spacing of bracing system. It could be seen from Figure 1 that induced maximum wall movement could be interpreted by excavation depth,  $S$  and  $F_b$ . Further, having the same  $S$  and excavation depth, the greater  $F_b$  leads to smaller wall movement.

### 2.3 TORSAL program

TORSA is a one-dimensional numerical program which considers the behavior of retaining wall as a beam resting upon an

elastoplastic foundation but is not capable to simulate the 3-dimensional behavior of deep excavation that use auxiliary measurements. However, a simplified approach was developed in order to transform the effects of buttress wall and cross wall into changing soil strength parameters based on the system stiffness, which allows the designers to incorporate the complex effects of buttress wall and cross wall in 1-dimensional excavation analysis. Details of simplified approach are described by Hsieh and Lu (1999). The same approach was adopted in order to conduct analyses using TORSA in this study.

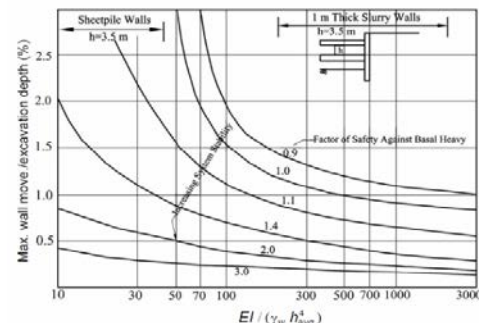


Figure 1 Relationship between maximum wall movement and system stiffness (after Clough et al. 1989)

### 2.4 PLAXIS 3D program

PLAXIS 3D is a finite element program intended for three-dimensional analysis of deformation and stability in geotechnical engineering. In three-dimensional model, it can consider three-dimensional effect, like buttress wall and cross wall. A 3D FEM model of excavation site was used and the Mohr-Coulomb soil model was applied in analysis. The length, width and depth of the model is 120 m, 120 m and 59.9 m, respectively, as presented in Figure 2.

## 3. CASE HISTORY

### 3.1 Site description

Case A is a 17-story office building with 4 basement levels. The project site is about 40 m in length 38 m in width and 59.9 in depth, and the excavation depth of the basement is 17.1 m. Diaphragm wall is 0.8 m in thickness and 34 m in depth together with 5 levels of H-steel bracing as the retaining system. The typical horizontal spacing of H-steel bracing is 6 m, and each level of bracing was preloaded to 50% of its allowable axial capacity. The depth of the cross wall

extends from GL.-16 m to GL.-34 m. There are six inclinometer casings installed in the perimeter diaphragm wall as shown in Figure 3. The ground water level was at 2 m below surface level.

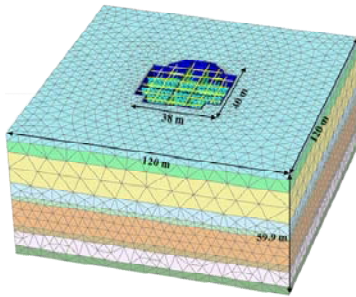


Figure 2 The model used for 3D FEM analyses

### 3.2 Wall displacement of field observation

The wall displacement measured from 4 selected inclinometers, SID-1, SID-3, SID-4 and SID-5 are used for further evaluation and locations of these inclinometers are shown in Figure 3. The depth of toe of these inclinometers are installed at the same depth of wall toe. Unfortunately, only data at final excavation stage are available for comparisons and details are drawn in Figure 4. It is realized that SID-5 had the largest wall displacement, was 7.762 mm, and the depth of maximum wall displacement was at G.L.-10 m to G.L.-11 m. The maximum wall displacement of SID-3 was about 4.180 mm, and the depth of maximum wall displacement was at G.L.-10.65 m. Additionally, the wall moves outward instead of inward at SID-1 and SID-4. The maximum wall displacement of SID-1 and SID-4 were -3.433 mm and -5.056 mm, respectively, and the depth of

maximum wall displacement were G.L.-19.04 m and G.L.-1.63 m. In other words, the wall behavior at SID-1 and SID-4 were similar, and SID-3 was coincided with SID-5. As shown in Figure 3, both of SID-1 and SID-4 were installed in the wall which attached to cross wall. This might be the reason that the induced displacement could become very small but unlikely to move outward at final excavation stage. In contrast, the location of SID-3 and SID-5 were not close to the cross wall so the wall displacements were larger than SID-1 and SID-4.

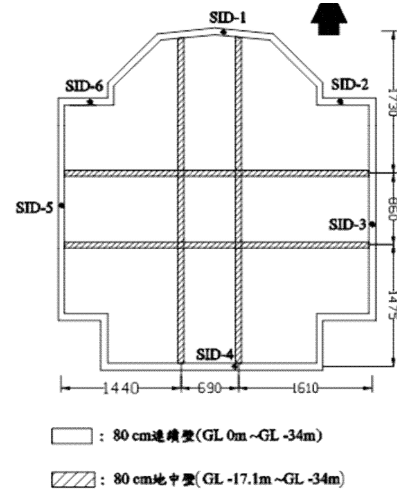


Figure 3 Layout of diaphragm wall and cross wall for Case

Table 1 Material properties of the soil layers

Layer	Type	Depth from m	Depth to m	$r_f$ kN/m <sup>3</sup>	SPT-N	$s_u$ kN/m <sup>2</sup>	$\phi'$ °	$\psi'$ °	$E$ kN/m <sup>2</sup>
1	CL	0	-3.5	18.7	5	54	0	0	27000
2	SM	-3.5	-9.3	20	8	0	31	0	16000
3	CL	-9.3	-24.2	18.6	3	32.4	27	0	16200
4	CL	-24.2	-30.4	18.6	6	74.5	30	0	37250
5	SM	-30.4	-32.8	18.7	9	0	31	0	18000
6	CL	-32.8	-45.4	18.3	10	98.1	31	0	49050
7	CL	-45.4	-48.4	18.2	15	107.9	0	0	53950
8	CL	-48.4	-56.1	19.1	19	135.4	0	0	67700
9	GM	-56.1	-59.9	21.6	>100	0	37	0	912000

Table 2 Bottom-up excavation sequence of Case A

Phase	Activity	Remarks
1	Excavation to GL.-1.7 m	First exc. Stage
2	Install strut at GL. -1.0 m	H300*300*10*15 mm Preload: 490kN/ea
3	Excavation to GL.-4.8 m	Second exc. Stage
4	Install strut at GL. -4.1 m	H400*400*13*21 mm Preload: 980kN/ea
5	Excavation to GL.-8.0 m	Third exc. Stage
6	Install strut at GL. -7.3 m	2H400*408*21*21 mm Preload: 980kN/ea
7	Excavation to GL.-11.2 m	Fourth exc. Stage
8	Install strut at GL. -10.5 m	2H400*408*21*21 mm Preload: 980kN/ea
9	Excavation to GL.-14.4 m	Fifth exc. Stage
10	Install strut at GL. -13.7 m	2H400*408*21*21 mm Preload: 980kN/ea
11	Excavation to GL.-17.1 m	Final exc. Stage
12	Cast B4FL and FS	at GL.-14.4 m and GL.-17.1 m
13	Remove the fifth floor support	
14	Cast B3FL	at GL.-11.2 m (t=40 cm)
15	Remove the fourth floor support	
16	Cast B2FL	at GL.-8.0 m (t=40 cm)
17	Remove the third floor support	
18	Cast B1FL	at GL.-4.8 m (t=40 cm)
19	Remove the first and second floor support	
20	Cast 1FL	at GL.0 m (t=25 cm)

Table 3 Material properties of the diaphragm walls, cross walls and basement floors

Parameters	Unit	Diaphragm Wall	Cross Wall (a)	Cross Wall (b)	F1	B1F	B4F	FS
D	m	0.8	0.8	0.8	0.25	0.4	0.2	0.6
r	kN/m <sup>3</sup>	5.65	5.65	5.65	0	0	0	0
f <sub>c</sub>	kN/m <sup>2</sup>	2.75E+07	1.37E+07	2.40E+07	2.75E+07	2.75E+07	2.75E+07	2.75E+07
E	kN/m <sup>2</sup>	2.46E+07	1.74E+07	2.30E+07	2.46E+07	2.46E+07	2.46E+07	2.45E+07
v <sub>12</sub>		0.2	0.2	0.2	0.2	0.2	0.2	0.2

Table 4 Material properties of the anchors

Parameters	Unit	H300x300	H400x400	2H400x408
Depth	m	-1	-4.1	-7.3, -10.5, -13.7
E	kgf/cm <sup>2</sup>	2.04E+06	2.04E+06	2.04E+06
A	cm <sup>2</sup>	118.4	218.7	501.4
EA	kN	2.37E+06	4.38E+06	1.00E+07
Preload	kN	490	980	980

stress analysis, as the clay layers are under undrained type C of total stress analysis due to limitation of available data from site investigation. As shown in Table 1, the effective Young's modulus of sand layers was determined by the following equation after Hsiung (2009).

$$E = 2000N(kPa) \quad (2)$$

where N is the number of standard penetration test (SPT). The undrained Young's modulus of clay layers was obtained by the following empirical equation as reported by Bowles (1996), Lim et al. (2010), Likitlersuang et al. (2013), Khoiri and Ou (2013).

$$E_u = 500_{su} (kPa) \quad (3)$$

where  $su$  is undrained shear strength of clay. The ground profile and cross section of the excavation are presented in Figure 5. As indicated in Figure 5, the excavation has to be delivered mostly in clay, very occasionally in thin layer of sand. Further, as indicated in Table 1, SPT-N of clay above final excavation level is less than 10 which is comparatively soft. By the same reason, additional cross wall is thus considered in order to restrain the wall movements induced. Parameter of structures, such as walls, floors and anchors are shown in Table 3 and Table 4. The excavation sequence of Case A is shown in Table 2, including the sizes and preloads of horizontal struts.

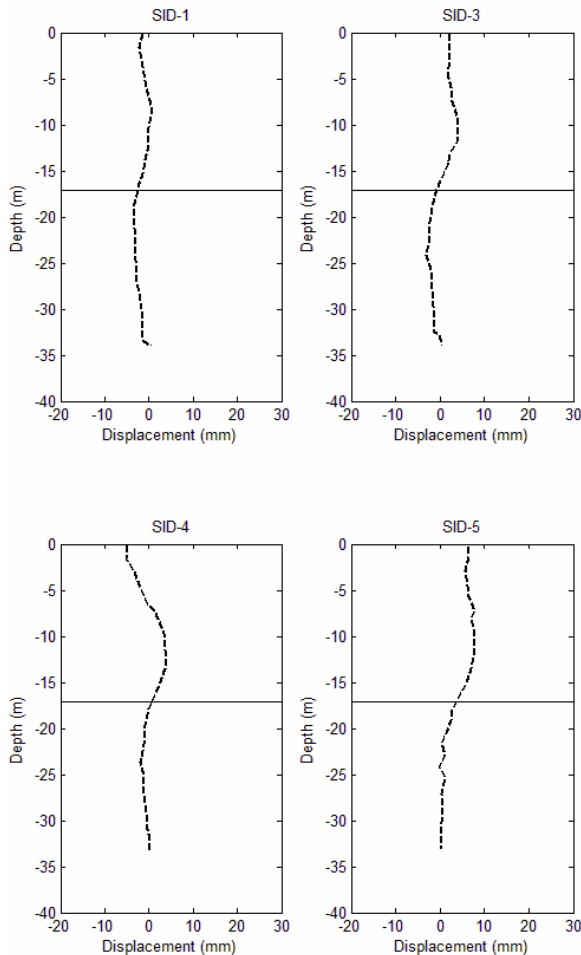


Figure 4 Wall displacements of field observation

## 4. RESULTS OF CASE HISTORY

### 4.1 PLAXIS 3D numerical model and material properties

Details of dimension of analytical model used are described previously and the excavation is approximately 40 m by 38 m. Soil properties of each layer are listed in Table 1 and elastic-perfect plastic Mohr-Coulomb model is chosen for ground behavior simulation. The sand layers are under drained condition of effective

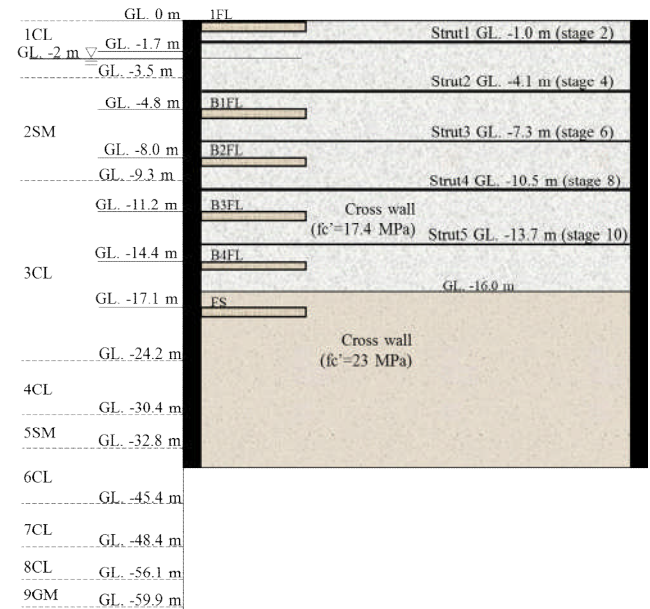


Figure 5 Soil stratigraphy and construction sequence for Case A

### 4.2 Results of PLAXIS 3D numerical analysis

The results of wall displacement of real 3D numerical analysis at final excavation stage at various locations are shown in Figure 6. It is realized that the wall displacement of above excavation level is larger than the wall displacement of below excavation surface. This might be connected with depth of cross wall as the cross wall was

constructed from one meter above final excavation level down to the same depth of the wall toe which expects to limit wall displacement at same depth. In general, the maximum wall displacement is less than 20 mm at final excavation stage which is insignificant. Additional corner effect formed by construction of cross wall also reduces the overall wall displacement, no matter the wall is attached by the cross wall directly or not.

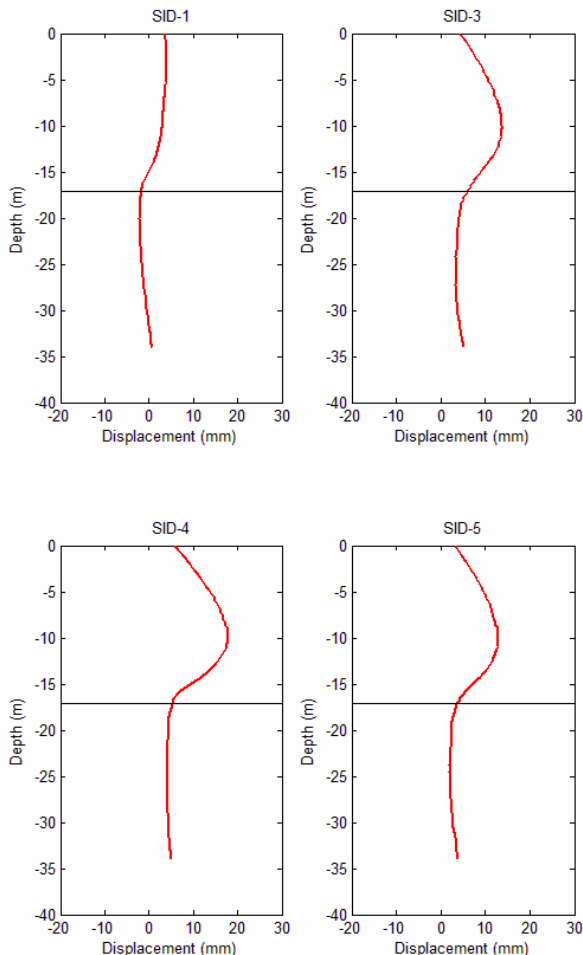


Figure 6 Wall displacements of PLAXIS 3D analysis at final excavation stage

#### 4.3 Compare with field observation

Wall displacement on each side of the site were analyzed by PLAXIS 3D and compared with field measurements, as shown in Figure 7. It is found that the results of PLAXIS 3D are slightly higher than field observation but the trend of entire wall displacement are close. Especially, the SID-1 is in a good agreement with field data. As SID-1 is located in the wall attached to the cross wall directly, the displacement is small and likely the inclinometer toe is fully fixed and it might be the reason that both observational data and analytical results can be consistent. Also shown in Figure 7, predictions of SID-3 and SID-5 indicate that wall/inclinometer toe shall have certain movements but toe is assumed to be fully fixed for field measurement. The field measurement may thus be underestimated due to toe movement and this might be the reason to lead the differences between analytical results and field observations.

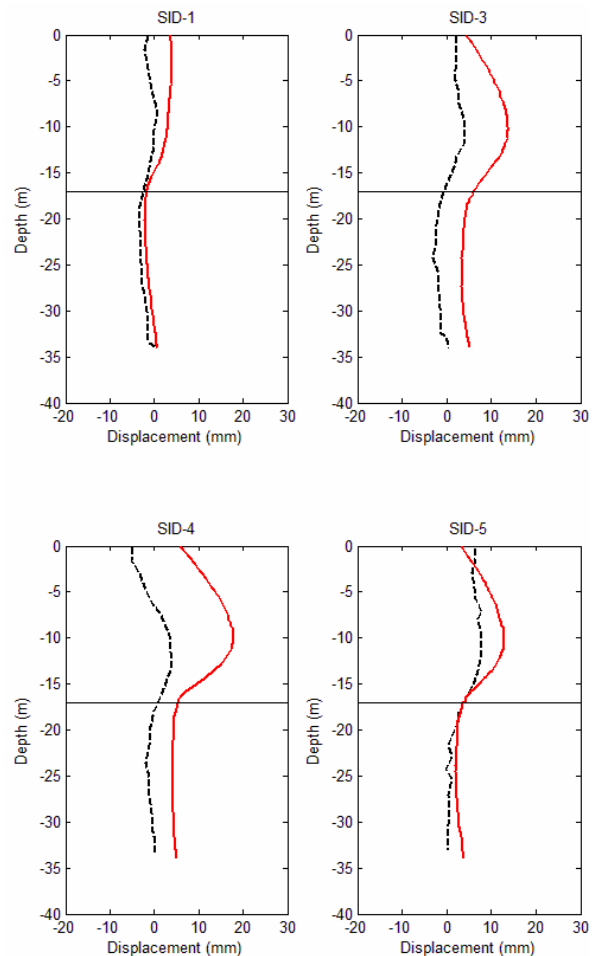


Figure 7 Compare the wall displacement of PLAXIS 3D and field observation

#### 4.4 Compare with the results of TORSAN numerical analysis

As stated above, due to limit of time and budget, one-dimensional analyses are widely adopted instead of real 3D FE analyses. That is the reason that a simplified approach has to be developed in case 3-dimensional characteristic of the excavation, such as cross-wall has to be simulated by one-dimensional analytical software.

Comparisons of analytical results of PLAXIS 3D and TORSAN together with field observations at final excavation are presented in Figure 7. It can be seen that PLAXIS 3D performs much better rather than TORSAN does. Because TORSAN, one-dimensional numerical program, has a limitation in modeling three-dimensional behavior of cross wall, though a simplified approach has been recommended.

It is also seen from Figure 8 that prediction of TORSAN shows the wall should move outward instead of inward during the excavation which is not very reasonable. It is thus suggested that there is still a space to discuss how to run TORSAN properly if additional cross wall has to be adopted in the excavation.

The maximum wall displacements of both analytical results and observations are shown in Table 5. The TORSAN simulated results are overestimated, as PLAXIS 3D results are much closer to the field data, while the observed maximum wall displacements are less than 10 mm. The ratio of the maximum wall movement to the excavation depth can vary from 0.05% (field measurement) to 0.15% (TORSAN analyses).

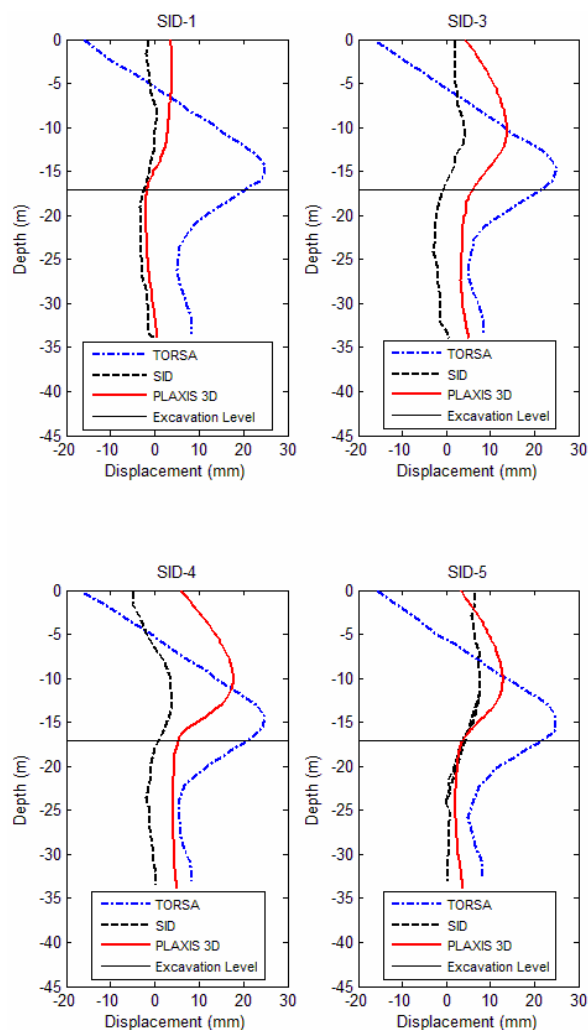


Figure 8 Comparisons of wall displacements from field measurements and analyses

Table 5 Comparisons of analytical results with field observation

Program	Max. wall displacement	Max. wall displacement/excavation depth
	mm	%
Field data	7.76119	0.045387
TORSA	25.1685	0.147184
PLAXIS 3D	17.77	0.103918

## 5. DISCUSSIONS

As described before, only data at final excavation stage are available, it is thus difficult to have a full discussion for an excavation in clay with additional cross wall. Through conclusions in Section 4.4, it is agreed that simulation using TORSA still has a room to be improved. Therefore, stage by stage deformations from real 3D analyses are selected for further discussions herein. The wall deformations of PLAXIS 3D analysis for each excavation stage are shown in Figure 9, 10 and 11, where the dash line is the depth of excavation surface. As further excavated, the wall deformation would become larger. The results of wall deformation of SID-3 and SID-5 are similar, with maximum wall displacements in the vicinity of 15 mm. However, it is obvious that the results of SID-1 are smaller than SID-3 and SID-5, and the maximum wall displacement is 4 mm. It might be attributed to an apparent corner effect at the location of SID-1.

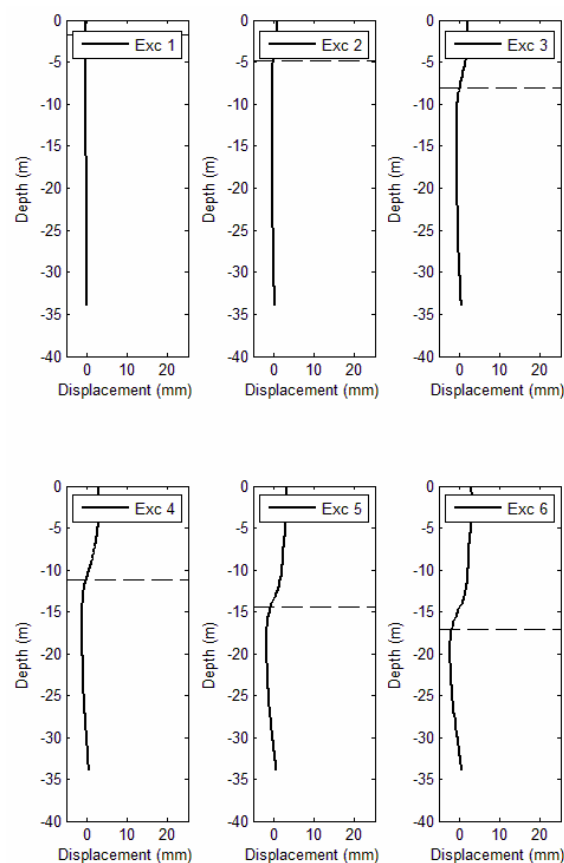


Figure 9 Wall displacement of SID-1

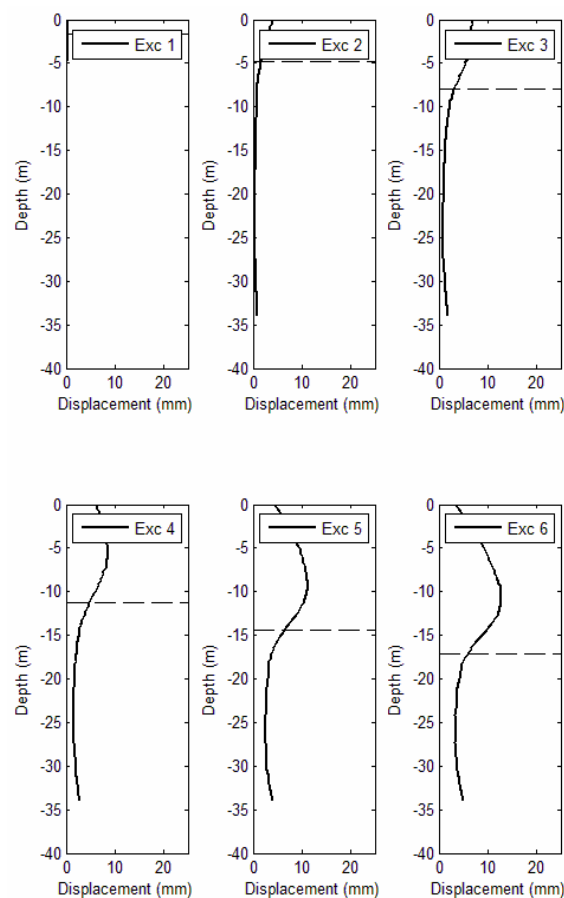


Figure 10 Wall displacement of SID-3



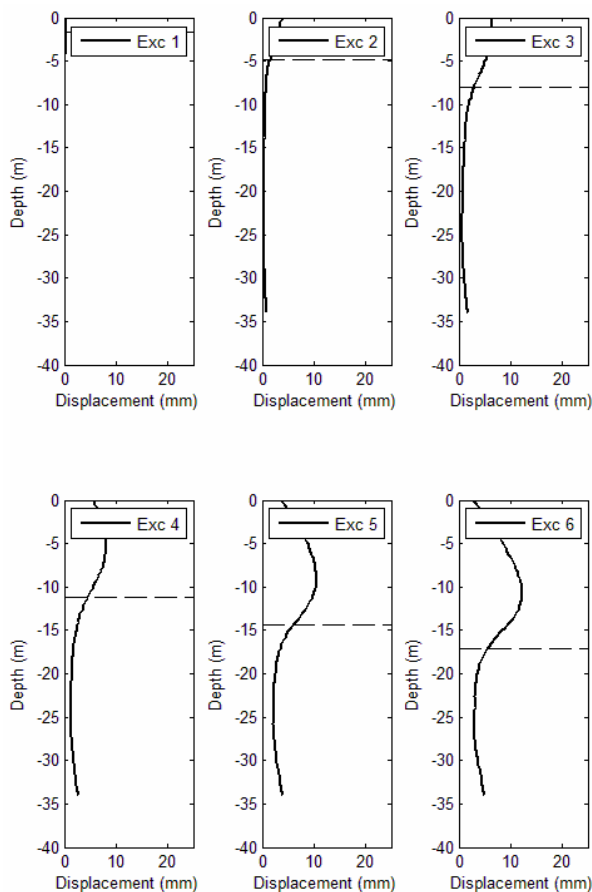


Figure 11 Wall displacement of SID-5

## 6. CONCLUSIONS

Through this study, following conclusions are made.

- (1) System stiffness (S) in excavation is an index which includes flexural stiffness of the retaining wall, the unit weight of water, and the average vertical spacing of bracing system.
- (2) By considering S, safety factor against basal heave (Fb) and excavation depth, the maximum wall displacement could be predicted. In addition, having the same S and excavation depth, larger Fb should lead to smaller displacement.
- (3) It is aware that wall displacement could be much smaller at the place once cross wall directly attached to it. However, the depth and height of cross wall also affect the magnitude and shape of wall displacement. The wall displacement might still be generated if there is no cross wall at said depth.

- (4) It is likely that a real 3D FE analyses can provide a reasonable prediction of wall displacements for an excavation with cross wall. The difference between observational data and analytical results might be caused by inclinometer toe movement.
- (5) Even though a simplified approach is provided, it still has a room to be improved if one-dimensional analytical software TORSAs has to be adopted to simulate wall displacement for an excavation with cross wall.

## 7. REFERENCE

- Terzaghi, K. (1967). *Theoretical Soil Mechanics*, John Wiley & Sons, New York.
- Clough, G.W., Smith, E.M., and Sweeney, B.P. (1989). "Movement control of excavation support systems by iterative design". *Proceedings, ASCE Foundation Engineering: Current Principles and Practices*, 2, 869-884.
- Ou, C.Y., Chiou, D.C., and Wu, T.S. (1996). "Three-dimensional finite element analysis of deep excavations". *Journal of Geotechnical Engineering, ASCE*, 122(5), 337-345.
- Finno, R.J., Blackburn, J.T., and Roboski, J.F. (2007). "Three-dimensional effects for supported excavations in clay". *Journal of Geotechnical and Geoenvironmental Engineering, ASCE*, 133(1), 30-36.
- Hsieh, H.S. and Lu, F.C. (1999). "A note on the analysis and design of diaphragm wall with buttresses". *Sino-Geotechnics*, 76, 39-50 (in Chinese).
- Hsieh, H.S. and Huang Y.H., Hsu, W.T. and Ge, L. (2017). "On the system stiffness of deep excavation in soft clay". *Journal of GeoEngineering*, Vol. 12, No. 1, pp. 21-34.
- Hsiung, B.C. (2009). "A case study on the behavior of a deep excavation in sand". *Computers and Geotechnics*, 36, pp. 665-675.
- Bowles, J.E. (1996). *Foundation analysis and design*, 5th Edition, McGraw-Hill Book Company, New York, USA.
- Khoiri, M. and Ou, C.Y. (2013). "Evaluation of deformation parameter for deep excavation in sand through case histories". *Computers and Geotechnics*, Vol. 47, pp.57-67.
- Lim, A., Ou, C.Y., and Hsieh, P.G. (2010). "Evaluation of clay constitutive models for analysis of deep excavation under undrained conditions". *Journal of GeoEngineering, TGS*, Vol. 5, No. 1, 9-20.
- Likitlersuang, S., Surarak, C., Wanatowski, D., Oh, E., and Balasubramaniam, A. (2013). "Finite element analysis of a deep excavation: a case study from the Bangkok MRT". *Soil and Foundations*, Vol. 53, No. 5, pp. 756-773.